Feigenbaum's Universality in a Low-Dimensional Fluid Model.

A. Meseguer, F. Marquès, J. Sánchez
Dep. Física Aplicada, Universitat Politècnica de Catalunya,
08034 Barcelona, Spain.

November 5, 2001

Abstract

We present a low-dimensional truncated model for a viscous fluid contained in a two-dimensional square box, obtained by truncating a dynamical system of amplitudes for the velocity field. This low-dimensional model exhibits a route to chaos via a period doubling cascade (Feigenbaum's Scenario). In order to compute with high accuracy the period doubling, a numerical method based on the first order variational equations and a Poincar map, has been developed. This methodology can also be applied to the analysis of bifurcations of periodic orbits in low dimensional ordinary differential equations. This method allows to detect not only the presence of bifurcations but also the computation of stable and unstable periodic orbits. On the other hand, the chaotic dynamics of the system is analyzed in detail by the computation of the Liapunov exponents for long-time integrations. For this purpose, a numerical scheme based on renormalization techniques has been constructed.

Key words: Feigenbaum's Universality, period doubling cascade, Poincar Map, Liapunov exponents, strange attractors.

Running title: Feigenbaum's Universality in a fluid model.

1 Introduction.

Low-dimensional analysis of fluid systems are of interest in order to capture the essential features of their behaviour. Many fluid dynamics problems have been analyzed from this point of view [Lorenz (1963)], [Boldrighini (1979)]. Of course, the results obtained from these models may not be directly related to experiment. However, they capture the basic qualitative features of the physical system. On the other hand, this kind of models usually provide relevant information about the core dynamics which governs the fluid motion.

In this paper we introduce a low-dimensional analysis for the flow of a viscous fluid contained in a square box whose boundary conditions have been previously regularized. This regularization is needed for the analiticity of the solutions near the boundaries. We use a spectral Legendre-tau scheme in primitive variables in order to obtain a dynamical system of amplitudes for the velocity field. By truncating the system up to order four, a relatively simple system of ordinary differential equations is obtained. Its analysis is the main subject of this paper. We have found the stationary solution at low Reynolds number using a continuation method. This solution loses stability at a Hopf bifurcation, and suffers a cascade of period doubling bifurcations. We have computed these period doubling with suitable accuracy using a method based on the first variational equations for the Poincar map. The methodology we have introduced has a wide range of applicability in low dimensional ordinary differential equations. This method allows to detect the successive period doublings and to compute not only the stable periodic orbits but also the unstable ones.

For the truncated system we obtain a period doubling scenario in the Reynolds interval [503.26, 512.468]. This period doubling cascade verifies Feigenbaum's universality. Beyond $Re = 512.468$ the system presents chaotic behaviour. This is reflected in the Liapunov exponents analysis and in the Fourier spectra of the time evolution. Also, the structure of the Poincar section of the attractor presents fractal features.

The paper is organized as follows. In Sec.2 we present a physical description of the problem and the truncated four dimensional model, and we compute the steady solution an its stability. In Sec.3 we introduce the Newton-variational method to detect the period-doubling scenario and we apply it to our model. The bifurcations are computed with great accuracy; the resulting cascade is presented in detail. Sec.4 is devoted to the study of

the chaotic zone. The Liapunov exponents are computed as a function of the Reynolds number, showing the chaotic behaviour of the orbits. Moreover, periodic windows are obtained inside the chaotic region. We also present the results of the Fourier spectra from time integrations of the dynamical system for different regions. Finally, a Poincar section of the strange attractor is visualized in order to analyze its self-similar structure.

2 Physical Description. The Model.

Our problem consists of a two-dimensional square box of length L_0 filled with an incompressible fluid, whose velocity is given on one box side, and zero on the remaining ones, the so called cavity flow. We adimensionalize the variables using $L_0/2$, $L_0/2\nu$ as the unit length and velocity, being ν the kinematic viscosity. The fluid domain is $\Omega = [-1,1] \times [-1,1]$, in Cartesian coordinates (x, y). The boundary conditions are:

$$\vec{v}(\pm 1, y) = (0,0), \quad \vec{v}(x,-1) = (0,0), \quad \vec{v}(x,1) = \vec{v}_\Gamma = (R(x^2-1)^2, 0) \quad (1)$$

where R is the Reynolds number $R = L_0 v_0 / 2\nu$ and v_0 is the maximum of the imposed velocity on the side $y = 1$. We have taken a regularized velocity profile giving a continuous boundary condition on $\partial\Omega$ [Peyret (1983)].

The problem will be approximated in a weak spectral-scheme. The velocity field belongs to a free-divergence function space. Therefore, the incompressibility condition is automatically satisfied. On the other hand, the Navier-Stokes equation is projected over a space of solenoidal functions which verify suitable boundary conditions in order to annihilate the pressure term. The technical details of the method are explained in the Appendix.

The low-dimensional truncation of Navier-Stokes equations with the boundary conditions described in the previous section yields a four-dimensional dynamical system for the amplitudes.

$$\begin{pmatrix} \dot{u} \\ \dot{v} \\ \dot{w} \\ \dot{z} \end{pmatrix} = R \begin{pmatrix} -\lambda_1 \\ -\lambda_2 \\ 0 \\ 0 \end{pmatrix} + R^2 \begin{pmatrix} 0 \\ 0 \\ -\lambda_3 \\ -\lambda_4 \end{pmatrix} - \begin{pmatrix} d_1 & 0 & 0 & 0 \\ 0 & d_2 & 0 & 0 \\ 0 & 0 & d_3 & 0 \\ 0 & 0 & 0 & d_4 \end{pmatrix} \begin{pmatrix} u \\ v \\ w \\ z \end{pmatrix} +$$

$$R\begin{pmatrix} 0 & 0 & -\nu_1 & \nu_2 \\ 0 & 0 & -\nu_3 & -\nu_4 \\ -\delta_1 & \delta_2 & 0 & 0 \\ \delta_3 & \delta_4 & 0 & 0 \end{pmatrix}\begin{pmatrix} u \\ v \\ w \\ z \end{pmatrix} + \begin{pmatrix} \rho_1 uz - \rho_2 vw \\ \rho_3 uw - \rho_4 vz \\ \rho_5 wz - \rho_6 uv \\ \rho_7 u^2 + \rho_8 v^2 - \rho_9 w^2 - \rho_{10} z^2 \end{pmatrix} \quad (2)$$

The coefficients are numerical constants which can be found in the Appendix.

The previous equations are too complicated to find analytical expressions for the stationary points and their dependence on the Reynolds number R. Nevertheless, we find the steady solution numerically by a continuation method; see [Keller 1977]. The solution branch is sketched in Fig. 1. We have computed the eigenvalues of the Jacobian matrix over the solution branch as a function of the parameter R. For values of R less than 321.5 the eigenvalues have negative real part. For $R = 321.5$ one pair of eigenvalues crosses the imaginary axis with non-zero imaginary part. Thus, a Hopf bifurcation appears. The orbit generated by this bifurcation is stable over the interval [321.5, 503.26].

3 Period Doubling Scenario. The Newton–Variational Method.

We will write the system (2) as $\dot{x} = f(x, R)$ for the sake of simplicity, and let $\phi(t, x)$ be the solution of this system with x as initial condition ($\phi(0, x) = x$). In order to fix the stability and secondary bifurcations of the periodic orbit γ that appears in the Hopf bifurcation, we have used a Poincar map. Let Π_0 be a hyperplane transversal to γ in a point $x_0 \in \gamma$. The equation of Π_0 is $(x - x_0) \cdot \xi = 0$, where ξ satisfies the transversality condition $\xi \cdot f(x_0, R) \neq 0$. The Poincar map is given by

$$\begin{array}{rccl} P: & \Pi_0 & \longrightarrow & \Pi_0 \\ & x & \longrightarrow & P(x) = \phi(\tau(x), x) \end{array} \quad (3)$$

where the function $\tau(x)$, the time of fly needed to return to Π_0, is obtained from the equation $(\phi(\tau(x), x) - x_0) \cdot \xi = 0$. The eigenvalues of DP give the stability of the periodic orbit γ. DP is the restriction to Π_0 of the solution of the first variational equation

$$\dot{J} = D_x f(\phi(t, x_0), R) J \quad , \quad J(0) = \mathbf{1}_4 \quad (4)$$

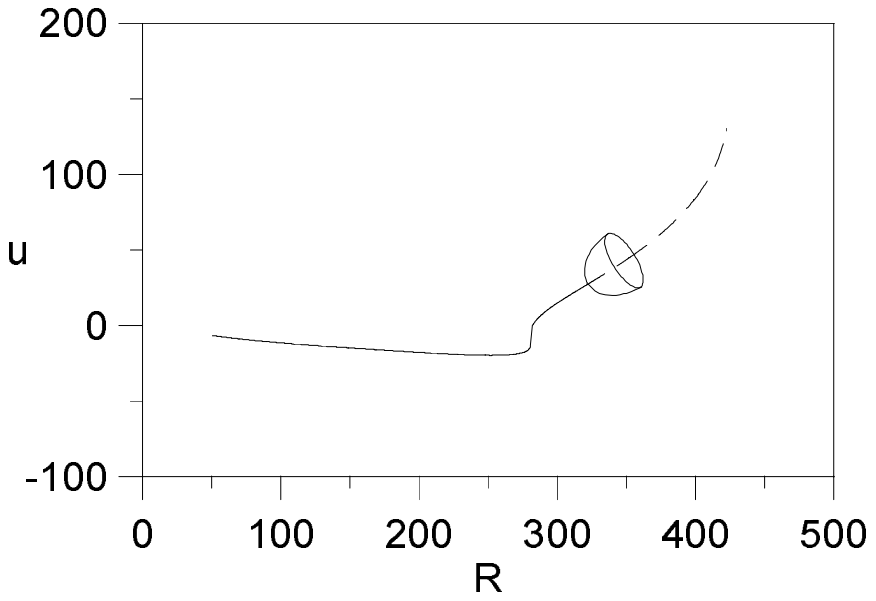

Figure 1: The fixed point as a function of the Reynolds number R. Solid line means stable, and dashed line, unstable. The parabolic shape that emerges from the continuous line represents the periodic orbit generated by the Hopf bifurcation.

where $\mathbf{1}_4$ is the identity matrix in $\mathbb{R}^4$. The projection on Π_0 is given by

$$DP = (\mathbf{1}_4 - \frac{f(x_0, R) \otimes \xi}{f(x_0, R) \cdot \xi}) J \mid_{\Pi_0} \tag{5}$$

DP is a 3×3 matrix.

The method we have termed Newton–variational is an iterative method that gives us simultaneously the periodic orbit, its period and the differential of the corresponding Poincar map. From an initial point x^k near to γ and an estimate T^k of the period, we integrate the system

$$\begin{array}{lll} \dot{x} = f(x, R) & , & x(0) = x^k \\ \dot{J} = [D_x f(x, R)] J & , & J(0) = \mathbf{1}_4 \end{array} \tag{6}$$

Next we refine the period by integrating the dynamical system (6) up to a final time $t = T^{k+1}$ that verifies the cut with the Poincar section:

$$(\phi(T^{k+1}, x^k) - x^k) \cdot \xi = 0 \tag{7}$$

This time can be obtained iteratively by linear interpolation or the bisection method. After that, we have a final point $x^{k+1/2}$, the Jacobian matrix and DP at this time T^{k+1}:

$$\begin{array}{l} x^{k+1/2} = \phi(T^{k+1}, x^k), \quad J^{k+1} = J(T^{k+1}) \\ DP^{k+1} = (\mathbf{1}_4 - \frac{f(x^k;R) \otimes \xi}{f(x^k;R)} \cdot \xi) J^{k+1} \mid_{\Pi_k} \end{array} \tag{8}$$

The last step of the iteration is the corrector Newton process in Π_k:

$$x^{k+1} = x^k + (\mathbf{1}_3 - DP^{k+1})^{-1} (x^{k+1/2} - x^k) \tag{9}$$

The matrix $\mathbf{1}_3 - DP^{k+1}$ must be invertible, i.e., its eigenvalues must be different from 1. But when γ is stable, the eigenvalues have moduli less than 1, and the bifurcations we have found are period doubling ones. The critical eigenvalue crosses the unit circle by -1 and the matrix of the Newton method is invertible. For $k \to \infty$, x^k gives a point of the orbit, regardless of whether it is stable or not. T^k and DP gives its period and eigenvalues.

This iterative method is the core of a continuation method in the Reynolds number R. We start with a R value at which γ is stable and obtain the first orbit by time evolution of (2). For a new value of R the iteration begins

with a point and the period of the previous orbit; if the orbit suffers a period doubling bifurcation, the new orientative period will be twice the former period.

The vector ξ is constant throughout the process, in order to simplify the calculations and always use the same coordinates for Π_0. The transversality to γ is ensured by moving x_0 along the orbit to a point p_γ where the angle between the orbit and the Poincar Map is maximum:

$$\frac{f(x,R)\cdot\xi}{\|f(x,R)\|\|\xi\|} \leq \frac{f(p_\gamma,R)\cdot\xi}{\|f(p_\gamma;R)\|\|\xi\|} \quad \forall x \in \gamma \tag{10}$$

By gradually varying the Reynolds number R we can determine with a high degree of accuracy (by successive linear interpolation, for example) the bifurcating values of R. We have found a period doubling cascade, whose first nine period doubling bifurcation values can be seen in Table 1. The table also shows the ratios between the successive bifurcation intervals, defined by:

$$\delta^n = \frac{R^{n+1}-R^n}{R^{n+2}-R^{n+1}} \tag{11}$$

We can observe that these ratios approach Feigenbaum's universal constant $\delta_F = 4.66920160\ldots$. The R^n sequence has an accumulation point at $R^\infty = 512.468014489$.

The first one, two, four and eight periodic states are sketched in Fig. 2, where we have represented the amplitude z versus the amplitude v.

4 Properties of the Strange Attractor.

Liapunov exponents give us information about the stability of the orbits and the long-term behaviour of the volume elements in phase space (i.e., contraction and expansion). For our problem we consider again the first order variational dynamical system

$$\begin{array}{lll} \dot{x} = f(x,R) & , & x(0) = x_0 \\ \dot{J} = [D_x f(x,R)]J & , & J(0) = \mathbf{1}_4 \end{array} \tag{12}$$

where now x_0 is a point of the orbit or the attractor to be considered, obtained after a suitable transient time integration. At every time we can compute

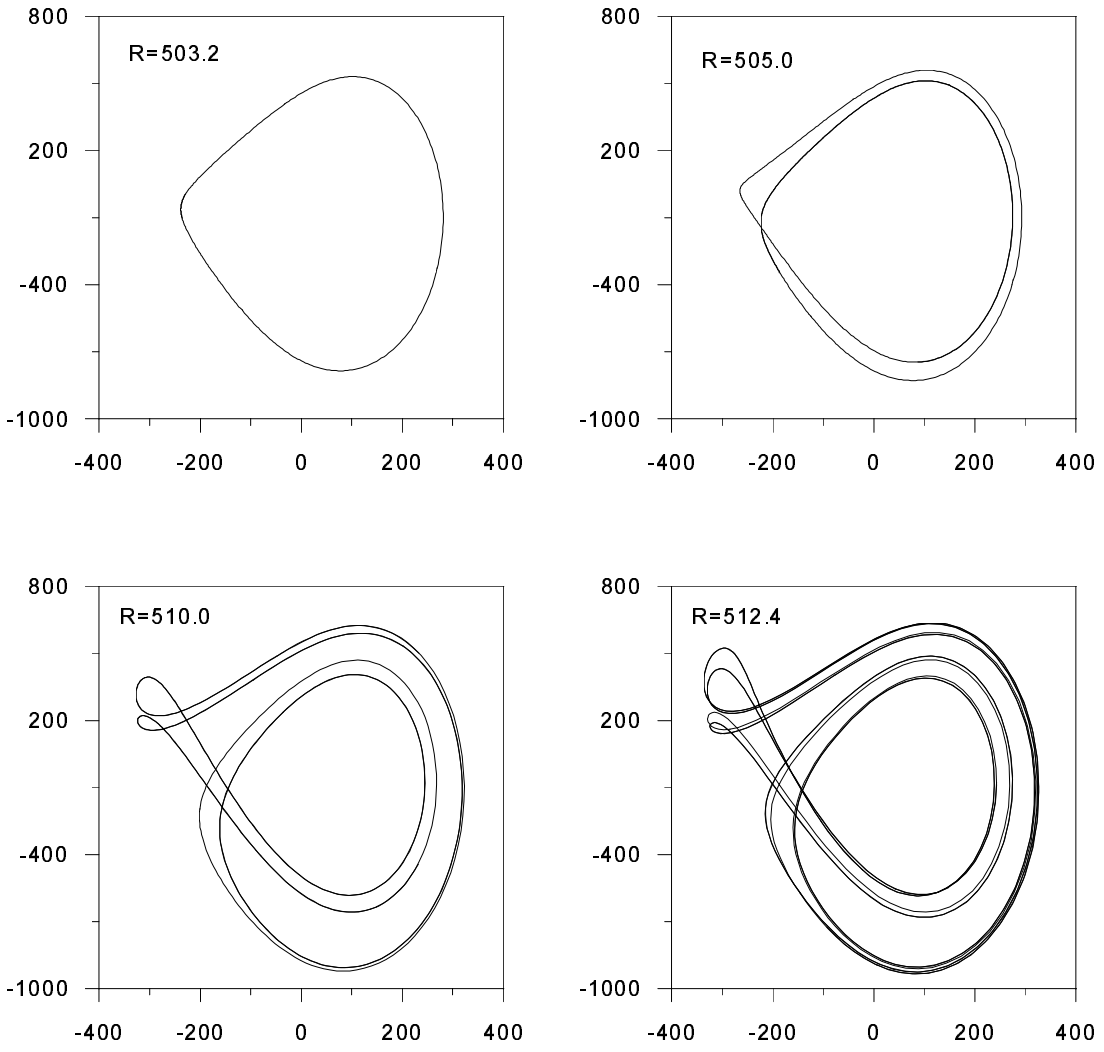

Figure 2: Orbits of the one, two, four and eight periodic states. In the figures the x axis corresponds to the v amplitude and the y axis to the z amplitude.

the eigenvalues μ_j of the matrix J. Then, the Liapunov exponents of our dynamical system will be:

$$\lambda_j = \lim_{T\to\infty} \frac{\log \mid \mu_j \mid}{T} \qquad (j = 1, 2, 3, 4) \tag{13}$$

When the Liapunov exponents are evaluated directly by integrating the first variational equations (12), numerical problems arise. The columns of $J(t)$ become almost parallel to the direction of the biggest Liapunov exponent, J becomes ill conditioned, and tends to be singular. Furthermore, if some of the Liapunov exponents are greater than zero, overflow problems can occur. Therefore, the previous limit cannot be computed directly. In order to handle this problem, we have used the renormalization method of Shimada and Nagashima [Shimada (1979)], described in [Kubicek (1983)]. We have computed the Liapunov exponents as a function of the Reynolds number. For the periodic solutions ($R \leq R^{\infty}$) we have a zero exponent and the remaining ones are less than zero, as it is well known. The behaviour of the greatest Liapunov exponent for $R > R^{\infty}$ is displayed in Fig. 3. Positive values of the exponent correspond to chaotic solutions, and we see that the system is chaotic but presents a window with a periodic stable solution. This behaviour is typical of many dynamical systems that suffer a period doubling cascade. Also, the system exhibits strong hysteresis. Different initial conditions can lead to different solutions, periodic solutions or chaotic solutions.

The strange attractor corresponding to the chaotic zone ($R = 512.5$) is sketched in Fig. 4. We have computed a Poincar section in order to analyze its geometric structure. This section is depicted in Fig. 5 for $R = 512.5$. Its self-similarity structure, typical of strange attractors is apparent. The fractal dimension of the attractor has been computed using the numerical method of Grassberger and Procaccia [Grassberger 1983]. The computed dimension for $R = 512.5$ is $d = 1.5854$.

The Fourier spectra for two different Reynolds numbers are shown in Fig. 6. The first spectrum corresponds to a periodic orbit, and the second one is in the chaotic region. We notice that the former exhibits a broad-band noise, whose level is two or more orders of magnitude higher than in the periodic case. This is a typical signature of chaos. In the chaotic spectrum sharp peaks appear above the level of the noise. Similar types of spectrum have been observed by other authors [Kubicek 1983]. This type of spectrum is

R_{crit}	δ
R^1=503.26263580	
R^2=507.98889404	δ^1=1.113
R^3=512.23403718	δ^2=23.361
R^4=512.41575610	δ^3=4.3590
R^5=512.45743770	δ^4=5.0208
R^6=512.4657403824	δ^5=4.6436
R^7=512.4675281125	δ^6=4.6773
R^8=512.4679103180	δ^7=4.6689
R^9=512.4679921795	

Table 1: Critical Reynolds numbers R^n and ratios δ^n for the period doubling cascade.

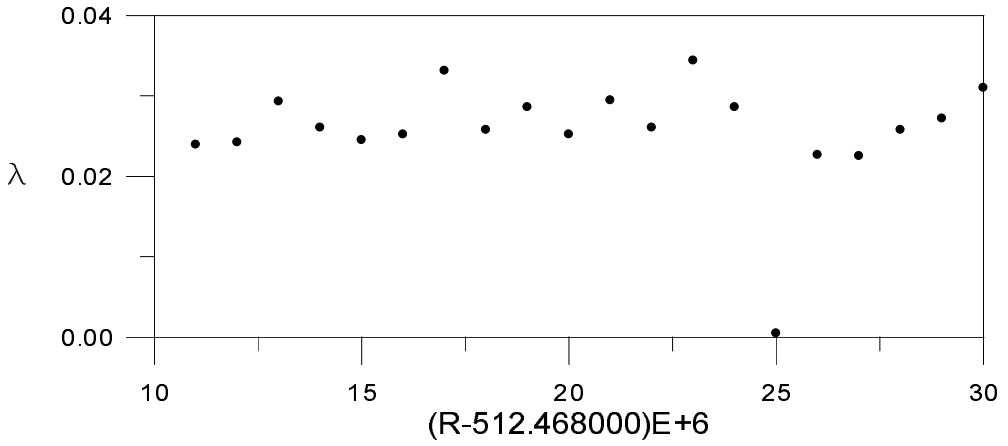

Figure 3: Maximum Liapunov exponent as a function of the Reynolds number R. Note the periodic solution at $R = 512.468025$

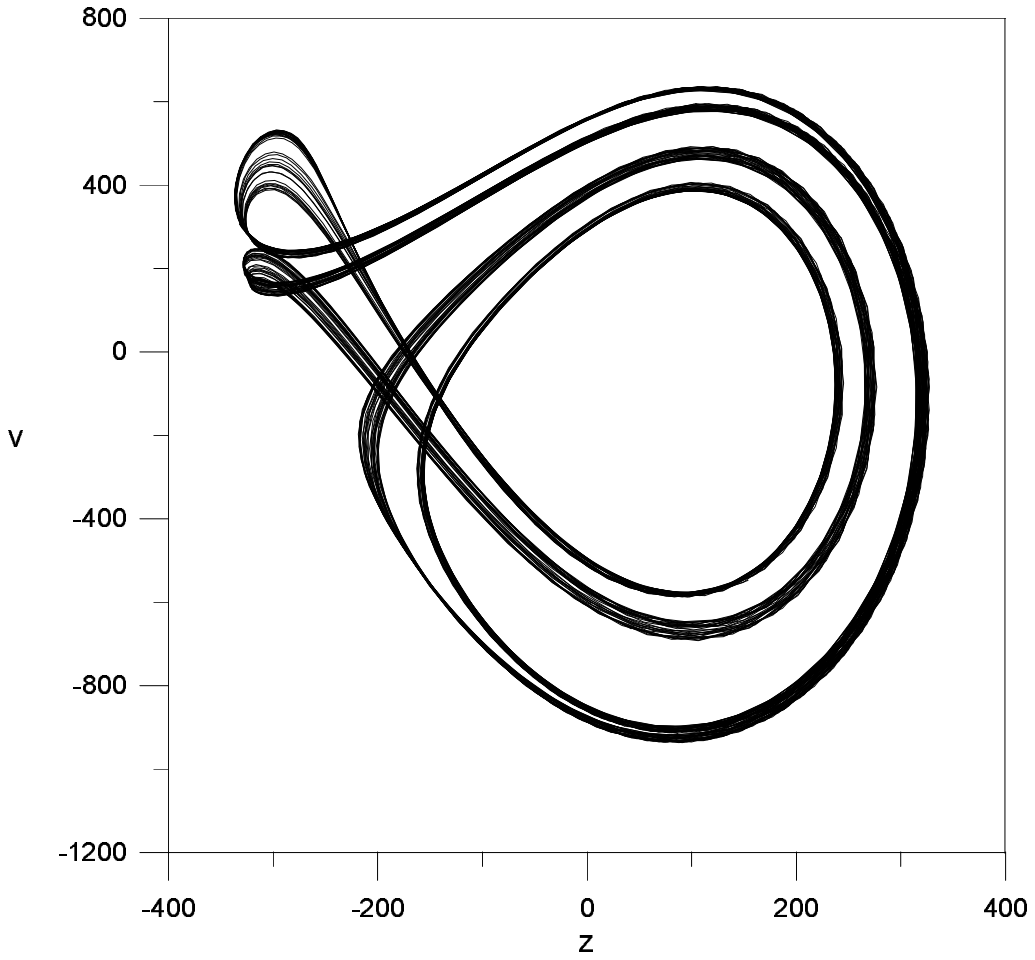

Figure 4: Plot of the strange attractor for $R = 512.5$. Projection into the plane (v,z).

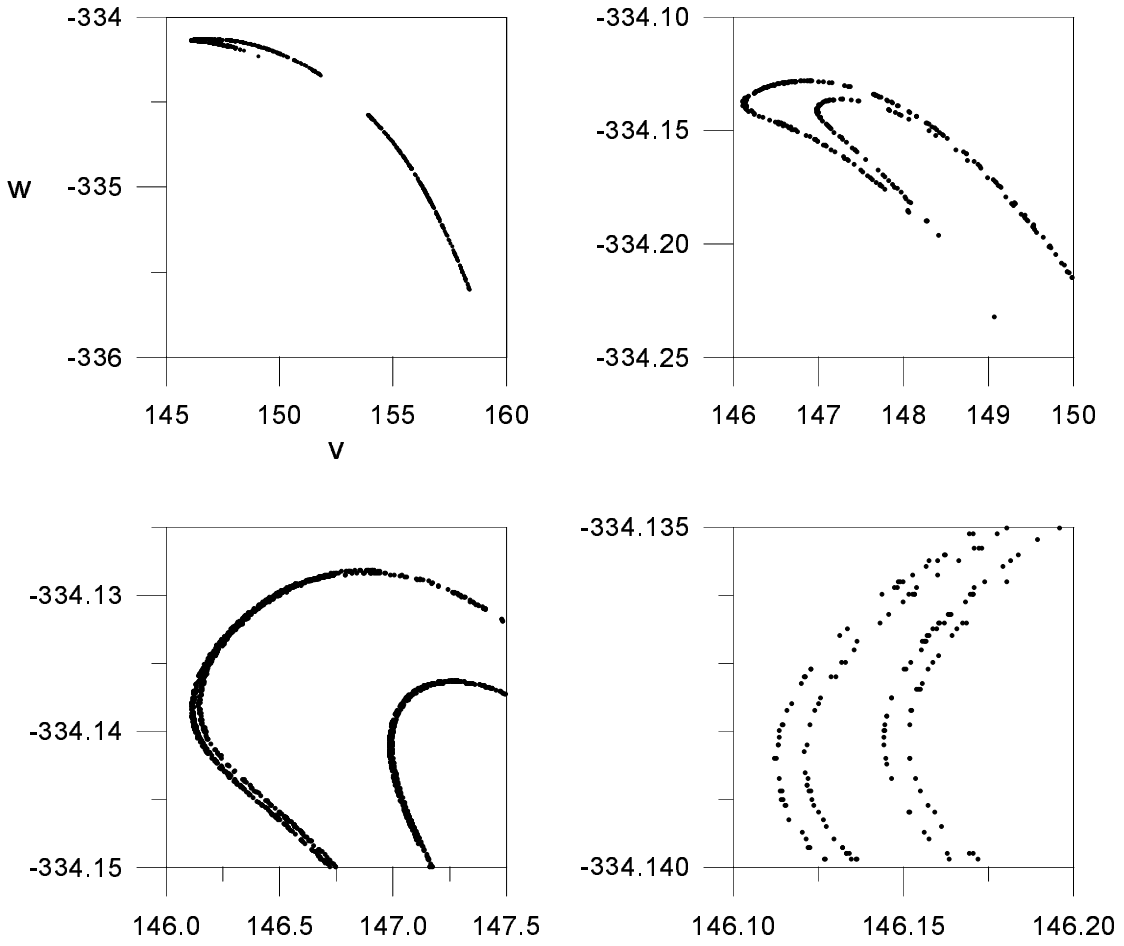

Figure 5: Poincar section of the strange attractor for $R = 512.5$. The enhanced areas show a self-similar structure. The variables displayed are (v, w)

called "phase coherent", and occurs close to unstable limit cycles generated by the sequence of period doubling bifurcations.

If we further increase the Reynolds number the chaotic attractor seems to collapse with the unstable manifold of another branch of steady solutions. This collision produces a destabilization of the attractor. This phenomenon is probably due to the excessive truncation of the model.

In order to check the behaviour of this low-dimensional model, we have obtained a six-dimensional system for the same problem, taking $M = 2$, $N = 3$ (see Appendix). The results obtained are very similar. The six-dimensional model also exhibits a period doubling scenario, although the bifurcations take place at different Reynolds numbers.

5 Conclusions.

By analyzing a truncated model for a two dimensional Navier-Stokes problem we find a transition to chaos by means of a period doubling cascade. The period doubling verifies Feigenbaum's universality. After the successive period doubling bifurcations, the system presents a chaotic behaviour. This is reflected in the Liapunov exponents and in the Fourier spectra of the time integrations of the dynamical system. A six-dimensional model has also been studied in order to check the results obtained with the four-dimensional one. In both cases, the qualitative phenomena are essentially the same. We have also introduced a useful methodology for the analysis of the bifurcations of periodic orbits in low dimensional ordinary differential equations, that we have termed the Newton-variational method.

Acknowledgements.

This work was supported by the Direccin General de Investigacin Cientfica y Tcnica (DGICYT), under grant PB94/1209. Dr. D. Crespo is thanked for his help in computing the fractal dimension of the attractor.

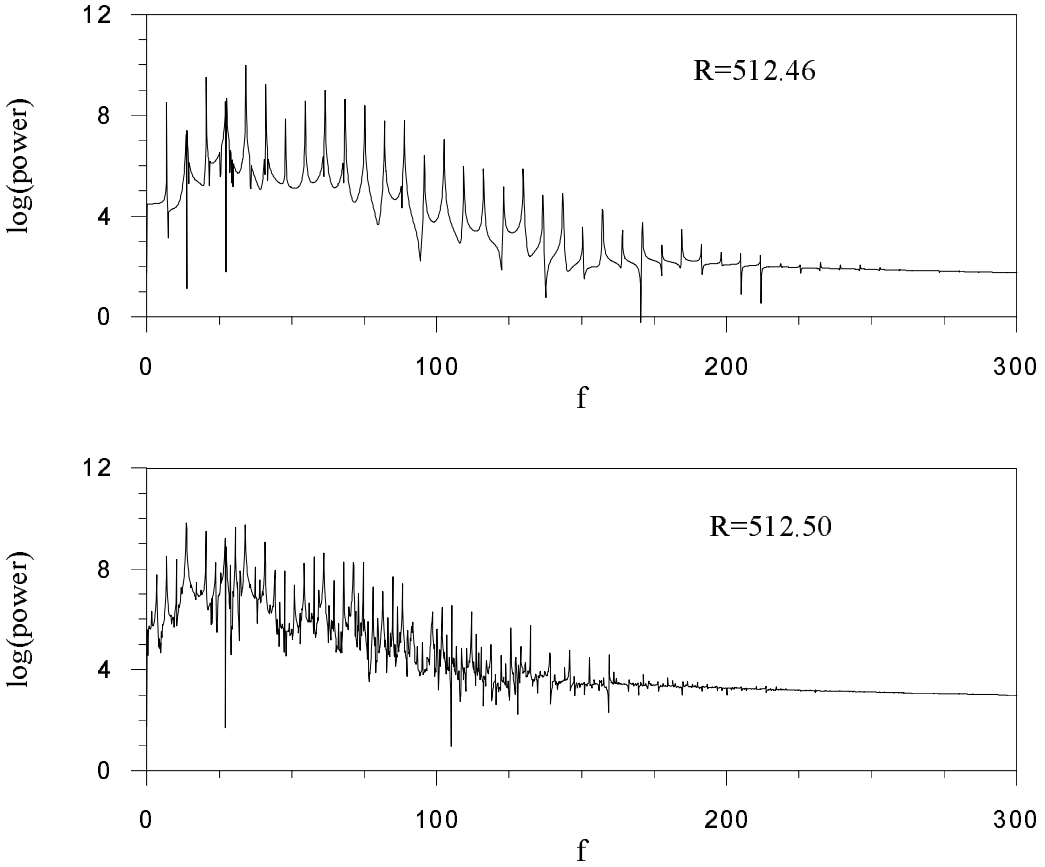

Figure 6: Fourier spectra for a periodic solution ($R = 512.46$) and a chaotic solution ($R = 512.50$).

Appendix.

We consider the adimensionalized Navier-Stokes equations for incompressible fluids:

$$\partial_t \mathbf{v} + (\mathbf{v} \cdot \nabla)\mathbf{v} = -\nabla p + \Delta \mathbf{v} \quad , \quad \nabla \cdot \mathbf{v} = 0 \tag{14}$$

In order to build a weighted residual scheme we will work with two different function spaces. Let H_d be the projection space of test functions:

$$H_d = \{\tilde{\phi} \in L^2(\Omega),\ \nabla \cdot \tilde{\phi} = 0,\ \tilde{\phi} \cdot \hat{n} \mid_{\partial\Omega} = 0\} \tag{15}$$

where $\hat{n}$ is the unit normal to $\partial\Omega$, and let H_s be the space of divergence-free functions:

$$H_s = \{\hat{\phi} \in L^2(\Omega),\ \vec{\nabla} \cdot \hat{\phi} = 0\} \tag{16}$$

Both spaces will be spanned by solenoidal functions $H_d = \text{Span} < \tilde{\phi}_{pq} >$, $H_s = \text{Span} < \phi_{mn} >$ of the form

$$\tilde{\phi}_{pq}(x,y) = \begin{pmatrix} -\tilde{f}_p(x)\tilde{g}'_q(y) \\ \tilde{f}'_p(x)\tilde{g}_q(y) \end{pmatrix} \quad , \quad \phi_{mn}(x,y) = \begin{pmatrix} -f_m(x)g'_n(y) \\ f'_m(x)g_n(y) \end{pmatrix} \tag{17}$$

where $'$ means derivative, and the normal component of $\tilde{\phi}_{pq}$ vanishes on the boundary $\partial\Omega$ of the domain: $\tilde{\phi} \cdot \hat{n} = 0$. These vectorial functions satisfy the divergence–free condition and are a base of the Hilbert spaces H_d and H_s respectively. Now the velocity field is of the form:

$$\mathbf{v}(x,y,t) = \sum_{m=0}^{M} \sum_{n=0}^{N} a_{mn}(t)\phi_{mn}(x,y) \tag{18}$$

The selection criteria of the set of functions $\tilde{\phi}_{pq}$ and ϕ_{mn} depend on the geometry of the problem and the boundary conditions. In fact, these functions will be built up using suitable orthogonal polynomials (see [Canuto (1988)] or [Moser (1983)] for a detailed discussion). We take the f and g functions as

$$\tilde{f}_p(x) = f_p(x) = (x^2-1)^2 P_p(x) \tag{19}$$

$$\tilde{g}_q(y) = g_q(y) = (y^2-1) P_q(y) \tag{20}$$

where P_p is the p^{th}-order Legendre polynomial. Thanks to the factors $(x^2-1)^2$ and y^2-1 the boundary conditions (1) are satisfied, except for the tangential

component on $y = \pm 1$. This remaining boundary condition will be set by the tau method.

The weak form of problem (14) will be

$$< \tilde{\phi} \mid \partial_t \mathbf{v} + (\mathbf{v} \cdot \nabla)\mathbf{v} - \Delta \mathbf{v} >= 0 \quad , \quad \forall \tilde{\phi} \in H_d,\ \mathbf{v} \in H_s \tag{21}$$

where $< \cdot \mid \cdot >$ is the standard Hermitian product. The pressure term $< \tilde{\phi} \mid \nabla p >$ vanishes for all $\tilde{\phi} \in H_d$ [Temam (1988)]. When the remaining boundary conditions are set, the coefficients a_{mn} are no longer independent. In fact we can find $a_{m,N}$, $a_{m,N-1}$ in terms of the remaining $a_{m,n}$, for all m. From Eq. (1),

$$a_{m,n} = -\frac{R}{4}\delta_{m,0} - \sum_{k=1}^{[n/2]} a_{m,n-2k}\ ; \qquad n = N,\ N-1\ ; \quad m = 0 \div M \tag{22}$$

corresponding to the imposed velocity profile $v(x) = R(x^2-1)^2$ on $y = 1$. The Eqs. (21) for the independent amplitudes in the case $N = 3$, $M = 1$ are Eqs. (2), where $u = a_{00}$, $v = a_{01}$, $w = a_{10}$ and $z = a_{11}$. The values of the numerical constants that appear in the Eqs. (2) are:

$$\begin{array}{llll}
\lambda_1 = 133/64 & \lambda_2 = 573/80 & \lambda_3 = 991/20592 & \lambda_4 = 73/5720 \\
\nu_1 = 23/2904 & \nu_2 = 1615/113256 & \nu_3 = 703/15730 & \nu_4 = 685/9438 \\
d_1 = 483/32 & d_2 = 267/8 & d_3 = 2003/80 & d_4 = 1521/40 \\
\delta_1 = 499/1716 & \delta_2 = 5/396 & \delta_3 = 801/1430 & \delta_4 = 17/26 \\
\rho_1 = 380/1573 & \rho_2 = 760/4719 & \rho_3 = 4776/7865 & \rho_4 = 280/1573 \\
\rho_5 = 12/143 & \rho_6 = 620/429 & \rho_7 = 504/715 & \rho_8 = 240/143 \\
\rho_9 = 1296/3575 & \rho_{10} = 72/1859 & &
\end{array} \tag{23}$$

References

[1] C. Boldrighini, V. Franceschini. *A five-dimensional Truncation of the Plane Incompressible Navier-Stokes Equations.* Commun. Math. Phys. **64**, 159-170 (1979).

[2] C. Canuto, M.Y. Hussaini, A. Quarteroni, T.A. Zang. *Spectral Methods in Fluid Dynamics.* Springer-Verlag (Springer Series in Computational Physics) (1988).

[3] P. Grassberger, I. Procaccia. *Characterization of Strange Attractors.* Phys. Rev. Lett. 50,346 (1983).

[4] H.B.Keller. *Numerical Solution of bifurcation and nonlinear eigenvalue problems* in Applications of Bifurcation Theory, edited by P.H. Rabinowitz. Academic, New York, 1977.

[5] M. Kubicek, M. Marek. *Computational Methods in Bifurcation Theory and Dissipative Structures.* Springer-Verlag (Springer Series in Computational Physics) (1983).

[6] E.N. Lorenz. *Deterministic Non-Periodic Flows.* J. Atm. Sci. **20** (1963), 130-141.

[7] R.D. Moser, P. Moin, A. Leonard. *A spectral numerical method for the Navier-Stokes equations with applications to Taylor-Couette Flow.* J. Comput. Phys. **52**, 524-544 (1983).

[8] R. Peyret, T.D. Taylor. *Computational Methods for Fluid Flow.* Springer-Verlag. (Springer Series in Computational Physics) (1983).

[9] I. Shimada, T. Nagashima. *A numerical approach to ergodic problem of dissipative dynamical systems.* Prog. Theor. Phys. **61** (1979), 1605-1615.

[10] R. Temam. *Infinite Dimensional Dynamical Systems in Mechanics and Physics.* Springer-Verlag. New York (1988).